

# COMPLETE SOLUTION OF NUCLEAR QUADRUPOLE–OCTUPOLE MODEL IN TWO DIMENSIONS\*

N. MINKOV

Institute of Nuclear Research and Nuclear Energy, Bulgarian Academy of Sciences  
Tzarigrad Road 72, 1784 Sofia, Bulgaria

M. STRECKER, H. LENSKE

Institut für Theoretische Physik der Justus-Liebig-Universität  
Heinrich-Buff-Ring 16, 35392 Giessen, Germany

*(Received November 10, 2015)*

A collective nuclear model of two-dimensional (2D) axial quadrupole–octupole (QO) vibrations coupled to rotations, originally restricted to coherent vibration modes allowing exact separation of variables and analytic solution of the eigenvalue problem, is developed beyond this restriction. The complete 2D problem is solved by diagonalizing the unrestricted QO Hamiltonian in the basis of the analytic solution. The test calculation for  $^{152}\text{Sm}$  showed that in this way the model description of yrast alternating-parity levels and the attendant  $B(E1)$ – $B(E3)$  transition probabilities is considerably improved compared to the coherent-mode case. At the same time, the shape of the QO potential is unambiguously determined providing model estimates for the quadrupole and octupole deformations of the nucleus.

DOI:10.5506/APhysPolBSupp.8.619

PACS numbers: 21.60.Ev, 21.10.Re, 23.20.-g, 27.70.+q

## 1. Introduction

The manifestation of complex shape effects in atomic nuclei is indicated by the specific structure of observed energy spectra and the attendant electromagnetic transitions. In particular, the appearance of alternating-parity bands (APBs) in even–even nuclei and quasi parity-doublet (QPD) sequences in odd mass nuclei is considered as the result of the presence of quadrupole–octupole (QO) deformations [1]. Usually, these spectra are attended by enhanced electric E1 and E3 transitions between levels with the opposite

---

\* Presented at the XXII Nuclear Physics Workshop “Marie and Pierre Curie”, Kazimierz Dolny, Poland, September 22–27, 2015.

parity. The leading collective mode associated with these shapes is the QO vibration on top of which rotation modes are built. In actinide nuclei, such as U and Pu and some rare-earth isotopes like Nd, Sm, Gd and Dy, the APBs do not form single octupole bands but rather indicate the presence of a soft QO mode in the collective motion. In many odd-mass nuclei, the coupling of the odd nucleon to the QO deformed core leads to the appearance of a QPD structure of the spectrum which can be also associated with soft-shape QO oscillations of the even–even core.

A collective model for nuclei with soft QO degrees of freedom was proposed in [2]. It is assumed that the shape of the system simultaneously oscillates in a 2D potential with respect to axial quadrupole and octupole deformation variables. The potential possesses an infinite angular momentum-dependent core at the zero-deformation point. The consideration of such a collective mode is expected to provide rich and interesting dynamical properties of the nuclear vibration–rotation motion. However, though looking relatively simple, the general 2D treatment of the eigenvalue problem appears to be far not trivial. In [2], it was shown that if certain relations between the quadrupole and octupole mass, stiffness and inertia parameters are imposed, the 2D problem can be reduced to a one-dimensional one for which a simple analytic solution can be obtained. The specifically assumed relations correspond to the imposition of a common, coherent oscillation frequency for the quadrupole and octupole vibration modes. It appeared that the analytic model formalism based on this coherent quadrupole–octupole mode (CQOM) quite reasonably describes the structure of yrast and non-yrast APBs and QPDs and the attendant  $B(E1)$ – $B(E3)$  transition probabilities in wide ranges of even–even and odd-mass nuclei [2–5]. Nevertheless, the imposed coherent constraints lead to certain limitations in the geometric interpretation of the physical pattern, such as the consequent ellipsoidal bottom of the QO deformation potential as well as some restrictions on the model descriptions due to the imposed purity of the coherent QO modes. To overcome these limitations, one has to solve the complete unrestricted 2D problem for the coupled QO vibrations and rotations. The aim of the present work is to show how this can be done by using the analytic solution from the constrained CQOM approach as a basis. It will be seen that the diagonalization of the unconstrained QO Hamiltonian in this basis provides a suitable way to solve the complete 2D problem. The solution avoids the singularity at the zero-deformation point and, in addition, benefits from the analytic form of the matrix elements obtained in ellipsoidal coordinates.

In Sec. 2, the QO model formalism and its CQOM limit are briefly presented. In Sec. 3, we explain the diagonalization procedure for the unconstrained Hamiltonian. In Sec. 4, a test result for the yrast APB of  $^{152}\text{Sm}$  is given and discussed. In Sec. 5, we briefly conclude.

## 2. Model of axial quadrupole–octupole vibrations and rotations

The QO model Hamiltonian  $H_{\text{QO}} = T_{\text{QO}} + U_{\text{QO}}$  is given by [2, 3]

$$T_{\text{QO}} = -\frac{\hbar^2}{2B_2} \frac{\partial^2}{\partial \beta_2^2} - \frac{\hbar^2}{2B_3} \frac{\partial^2}{\partial \beta_3^2}; \quad U_{\text{QO}} = \frac{1}{2}C_2\beta_2^2 + \frac{1}{2}C_3\beta_3^2 + \frac{X(I, K)}{d_2\beta_2^2 + d_3\beta_3^2}, \quad (1)$$

where  $\beta_2$  and  $\beta_3$  are axial quadrupole and octupole variables, respectively,  $B_2$  ( $B_3$ ),  $C_2$  ( $C_3$ ) and  $d_2$  ( $d_3$ ) are quadrupole (octupole) mass, stiffness and inertia parameters, respectively and

$$X(I, K) = \frac{1}{2} \left[ d_0 + I(I+1) - K^2 + \pi a \delta_{K, \frac{1}{2}} (-1)^{I+1/2} \left( I + \frac{1}{2} \right) \right]. \quad (2)$$

For even–even nuclei, one has  $X(I, K) = X(I, K=0)$ . The parameter  $d_0$  determines the potential shape at  $I=0$  and  $\pi$  is the total parity of the state. In odd-mass nuclei, the Coriolis decoupling factor  $a$  is considered for an odd-nucleon state with  $K=1/2$ . In the original work [3], this factor was taken as a model parameter and was adjusted to the experimental data. In later works [6, 7], it was calculated by using a reflection-asymmetric deformed shell model within a parity-projection particle-core coupling scheme.

The shapes of the potential  $U_{\text{QO}}$  are schematically illustrated in Figs. 1 and 2 in Ref. [2] where in Fig. 2, it is shown that under the constraint  $C_2/d_2 = C_3/d_3$  the potential possesses an ellipsoidal bottom. This implies the convenience of introducing ellipsoidal coordinates such that  $\beta_2 = p\eta \cos \phi$ ,  $\beta_3 = q\eta \sin \phi$ , with  $p = \sqrt{d/d_2}$ ,  $q = \sqrt{d/d_3}$  and  $d = (d_2 + d_3)/2$ . Then, the Hamiltonian appears in the form

$$\begin{aligned} T_{\text{QO}} = & -\frac{\hbar^2 d_2}{2dB_2} \left[ \cos^2 \phi \frac{\partial^2}{\partial \eta^2} + \frac{1}{\eta} \sin^2 \phi \frac{\partial}{\partial \eta} + \frac{1}{\eta^2} \sin^2 \phi \frac{\partial^2}{\partial \phi^2} \right. \\ & \left. + 2\frac{1}{\eta^2} \sin \phi \cos \phi \frac{\partial}{\partial \phi} - 2\frac{1}{\eta} \sin \phi \cos \phi \frac{\partial^2}{\partial \eta \partial \phi} \right] \\ & -\frac{\hbar^2 d_3}{2dB_3} \left[ \sin^2 \phi \frac{\partial^2}{\partial \eta^2} + \frac{1}{\eta} \cos^2 \phi \frac{\partial}{\partial \eta} + \frac{1}{\eta^2} \cos^2 \phi \frac{\partial^2}{\partial \phi^2} \right. \\ & \left. - 2\frac{1}{\eta^2} \sin \phi \cos \phi \frac{\partial}{\partial \phi} + 2\frac{1}{\eta} \sin \phi \cos \phi \frac{\partial^2}{\partial \eta \partial \phi} \right], \quad (3) \end{aligned}$$

$$U_{\text{QO}} = \frac{C_2 d \eta^2 \cos^2 \phi}{2d_2} + \frac{C_3 d \eta^2 \sin^2 \phi}{2d_3} + \frac{X(I)}{d\eta^2}. \quad (4)$$

Further, under the assumption of *coherent* QO oscillations with a frequency  $\omega = \sqrt{C_2/B_2} = \sqrt{C_3/B_3} \equiv \sqrt{C/B}$ , the collective energy of the system is obtained in the form [2, 3]

$$E_{nk}(I, K) = \hbar\omega \left[ 2n+1 + \sqrt{k^2 + bX(I, K)} \right], \quad n = 0, 1, 2, \dots; \quad k = 1, 2, 3, \dots, \quad (5)$$

where  $b = 2B/(\hbar^2 d)$ . The QO vibration wave function is

$$\Phi_{nkI}^\pm(\eta, \phi) = \psi_{nk}^I(\eta) \varphi_k^\pm(\phi), \quad (6)$$

where the “radial” part  $\psi_{nk}^I(\eta)$  involves generalized Laguerre polynomials in the variable  $\eta$  [2]. The “angular” part in the variable  $\phi$  is obtained under the boundary condition  $\varphi(-\pi/2) = \varphi(\pi/2) = 0$  which effectively reduces the solution to the case of  $\beta_2 > 0$  and provides a positive or negative parity,  $\pi_\varphi = \pm$ , of the wave function as follows:

$$\varphi_k^+(\phi) = \sqrt{2/\pi} \cos(k\phi), \quad k = 1, 3, 5, \dots \quad (\pi_\varphi = +), \quad (7)$$

$$\varphi_k^-(\phi) = \sqrt{2/\pi} \sin(k\phi), \quad k = 2, 4, 6, \dots \quad (\pi_\varphi = -). \quad (8)$$

The wave function for a state with angular momentum  $I^\pi$  belonging to an alternating-parity sequence in even–even nuclei has the form [2]

$$\Psi_{nIM0}^\pi(\eta, \phi) = \sqrt{\frac{2I+1}{8\pi^2}} D_{M0}^I(\theta) \psi_n^I(\eta) \varphi^\pi(\phi), \quad (9)$$

where  $D_{M0}^I(\theta)$  is the Wigner function. In odd–even nuclei the total core+particle wave function for a state with angular momentum  $I^\pi$  belonging to a parity-doublet sequence is given by [3]

$$\begin{aligned} \Psi_{nkIMK}^{\pi, \pi_{\text{sp}}}(\eta, \phi) = & \sqrt{\frac{2I+1}{16\pi^2}} \Phi_{nkI}^{\pi, \pi_{\text{sp}}}(\eta, \phi) [D_{MK}^I(\theta) \mathcal{F}_K \\ & + \pi \pi_{\text{sp}} (-1)^{I+K} D_{M-K}^I(\theta) \mathcal{F}_{-K}] , \end{aligned} \quad (10)$$

where  $\mathcal{F}_K$  and  $\pi_{\text{sp}}$  are the wave function and the parity of the single-particle state, respectively.

The energy spectrum of CQOM is determined in (5) by the quantum numbers  $n$  and  $k$ . In even–even nuclei, the APB is formed under the condition  $\pi(-1)^I = 1$ . Each band is characterized by a given  $n$  and a pair of odd and even  $k$ -values,  $k_n^{(+)}$  and  $k_n^{(-)}$  with  $k_n^{(+)} < k_n^{(-)}$ , corresponding to the positive- and negative-parity sequences, respectively. In odd-mass nuclei, the parity-doublet structure is imposed by the condition  $\pi = \pi_\varphi \pi_{\text{sp}}$ . Similarly to the even–even nuclei, the parity doublet is determined by a given  $n$  and a pair of odd and even  $k$ -values,  $k_n^{(+)}$  and  $k_n^{(-)}$  ( $k_n^{(+)} < k_n^{(-)}$ ). The  $k$ -values are determined so that  $k = k_n^{(+)}$  for  $I^\pi = \pi_{\text{sp}}^{(n)}$  and  $k = k_n^{(-)}$  for  $I^\pi = -\pi_{\text{sp}}^{(n)}$ , where  $\pi_{\text{sp}}^{(n)}$  is the parity of the ‘sp’ state on which the given QPD is built.

By using the CQOM formalism, the yrast and non-yrast APBs and QPBs and the attendant  $B(E1)$ ,  $B(E2)$  and  $B(E3)$  transition probabilities in various even–even and odd-mass nuclei were described [4, 5].

### 3. Diagonalization of the unconstrained QO Hamiltonian

The eigenvalue problem for Hamiltonian (1) with arbitrary values of the mass, stiffness and inertia parameters cannot be solved analytically and one has to search for a numerical solution. The standard way is to diagonalize the Hamiltonian in an appropriate basis. The obvious and most direct approach is to diagonalize (1) in the basis of a two-dimensional harmonic oscillator in the variables  $\beta_2$  and  $\beta_3$ . We have examined this possibility and found that essential difficulties come from the need to calculate the matrix elements numerically and even more, from the singularities in the numerical integrations in the zero deformation point ( $\beta_2 = \beta_3 = 0$ ). Then, we examined the possibility to diagonalize for given angular momentum  $I$  the Hamiltonian taken in ellipsoidal variables (3) and (4) in the basis of the analytic solution (6) obtained in the coherent mode assumption. In this case, the Hamiltonian matrix elements have the form

$$\langle n' k' | H | n k \rangle = \frac{d}{\sqrt{d_2 d_3}} \int_{-\frac{\pi}{2}}^{\frac{\pi}{2}} \int_0^\infty \psi_{n' k'}^I(\eta) \varphi_{k'}(\phi) H_{\text{QO}}(\eta, \phi) \psi_{n k}^I(\eta) \varphi_k(\phi) \eta d\eta d\phi, \quad (11)$$

where  $|n k\rangle \equiv \Phi_{n k I}^\pm(\eta, \phi)$ . By using the *Mathematica* program, we were able to obtain a lengthy, but well determined expression for the kinetic matrix element  $\langle n' k' | T_{\text{QO}} | n k \rangle$  in terms of products of matrix elements of powers of  $\eta$ ,  $\sin \phi$  and  $\cos \phi$ . Much simpler expression for the potential matrix element  $\langle n' k' | U_{\text{QO}} | n k \rangle$  directly comes from Eq. (4). Then, we get the matrix element (11) in a general form containing angular integrals of products of powers of  $\sin \phi$  and  $\cos \phi$  and integrals of the powers of  $\eta$ . The former are simplified and calculated with *Mathematica*, while the latter are easily calculated by using a known analytic expression for integrals involving two Laguerre polynomials [8]

$$\int_0^\infty t^{\alpha-1} e^{-pt} L_m^\lambda(pt) L_n^\beta(pt) dt = \frac{p^{-\alpha} \Gamma(\alpha) \Gamma(n - \alpha + \beta + 1) \Gamma(m + \lambda + 1)}{m! n! \Gamma(1 - \alpha + \beta) \Gamma(\lambda + 1)} \\ \times {}_3F_2(-m, \alpha, \alpha - \beta; -n + \alpha - \beta, \lambda + 1; 1), \quad (12)$$

where  ${}_3F_2$  denotes a generalized hypergeometric function. The function  ${}_3F_2$  is easily calculated through summation of its series representation. The use of the CQOM analytic basis has the following advantages:

- (i) Easily calculated analytic matrix elements;
- (ii) Built-in boundary condition and parity properties of the wave functions (see the text below Eq. (6));
- (iii) Avoiding the singularity at the zero deformation point. This feature of the basis wave functions is illustrated in Fig. 1 (right) showing how the density maxima surround the potential core at zero deformation in contrast to the 2D oscillator states, Fig. 1 (left). See also Fig. 3 in [2].

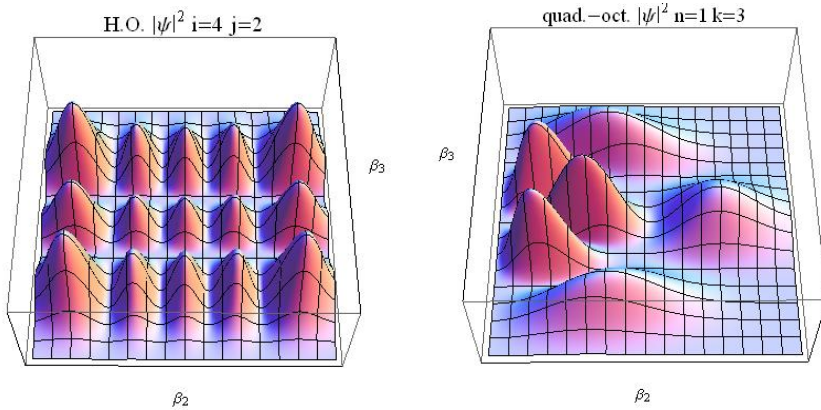


Fig. 1. (Color on-line) Schematic density plots for the 2D harmonic oscillator function (left) and the CQOM wave function (right) for  $\beta_2 \geq 0$  and  $-1 \leq \beta_3 \leq 1$ . The indices  $i, j$  and  $n, k$  denote numbers of oscillator quanta.

To get the spectrum, the Hamiltonian is diagonalized for each angular momentum  $I$  in a basis set of CQOM functions limited to large enough  $n$  and  $k$  oscillator-number values ensuring reliable eigenvalues and eigenfunctions at physically interesting (low) energies. The parameters of the basis are determined by taking into account the arithmetic average of the quadrupole and octupole mass and inertia parameters and, in addition, are optimized. The yrast APB or QPD band is determined by taking for each angular momentum  $I$  the lowest eigenvalue whose eigenfunction has the relevant parity. Each wave function is obtained in the form of an expansion

$$\tilde{\Psi}_I^\pi(\eta, \phi) = \sum_{n,k} C_{nkI} \Psi_{nkI}^\pi(\eta, \phi), \quad (13)$$

where the coefficients  $C_{nkI}$  are determined. Hence, the matrix elements of the electric transition operators are obtained in the form of sums over  $n$  and  $k$  of CQOM matrix elements. Thus, all reduced transition probabilities are calculated by using the formalism elaborated in the CQOM approach [4].

#### 4. Numerical result and discussion

Here, we illustrate the above approach in the yrast APB of the nucleus  $^{152}\text{Sm}$  for which CQOM descriptions were obtained in [2] and [4] (including non-yrast APBs). The parameters of the full unconstrained QO Hamiltonian (mass, stiffness and inertia parameters) were adjusted in order to reproduce the experimental levels and  $B(E1)$ – $B(E3)$  transition probabilities. The obtained parameters values are  $B_2 = 109.0\hbar^2/\text{MeV}$ ,  $B_3 = 100.08\hbar^2/\text{MeV}$ ,  $C_2 = 16.79 \text{ MeV}$ ,  $C_3 = 339.8 \text{ MeV}$ ,  $d_2 = 120.7\hbar^2/\text{MeV}$ ,  $d_3 = 4744\hbar^2/\text{MeV}$ ,  $d_0 = 81.40\hbar^2$  and effective charge  $e_{\text{eff}}^1 = 2.85e$  (see [4] for explanation). In Table I, the APB levels obtained in the present 2D QO model (2DQOM) are compared with those obtained in CQOM [2] and with the experimental levels [9]. The theoretical and experimental transition probabilities are compared in Table II. We see that the fits of the unconstrained Hamiltonian parameters essentially improve the APB description compared to CQOM, quality being measured by the standard root mean square (r.m.s.) value. Also the good description of transition rates is seen.

TABLE I

Theoretical 2DQOM and CQOM yrast APB levels (in keV) of  $^{152}\text{Sm}$  compared to experimental data [9].

$I^\pi$	CQOM	2DQOM	Exp.
	r.m.s. = 49 keV	r.m.s. = 33 keV	
1 <sup>−</sup>	853.73	889.20	963.354
2 <sup>+</sup>	112.23	109.00	121.782
3 <sup>−</sup>	994.59	1023.22	1041.114
4 <sup>+</sup>	357.52	350.25	366.479
5 <sup>−</sup>	1235.09	1252.12	1221.48
6 <sup>+</sup>	706.33	699.17	706.88
7 <sup>−</sup>	1557.94	1559.44	1505.61
8 <sup>+</sup>	1129.65	1129.51	1125.35
9 <sup>−</sup>	1945.59	1928.33	1879.11
10 <sup>+</sup>	1604.99	1618.84	1609.23
11 <sup>−</sup>	2382.93	2344.09	2326.96
12 <sup>+</sup>	2116.62	2149.75	2148.51
13 <sup>−</sup>	2857.99	2794.89	2833.25
14 <sup>+</sup>	2653.93	2708.84	2736.01

TABLE II

Theoretical (2DQOM) and experimental [10, 11] reduced transition probabilities for  $^{152}\text{Sm}$ .

Mult.	Transition	2DQOM [W.u.]	Exp. [W.u.]
E2	$2^+ \rightarrow 0^+$	139	144(3)
E2	$4^+ \rightarrow 2^+$	209	209(3)
E2	$6^+ \rightarrow 4^+$	251	245(5)
E2	$8^+ \rightarrow 6^+$	286	285(14)
E2	$10^+ \rightarrow 8^+$	316	320(3)
E1	$1^- \rightarrow 0^+$	0.0041	0.0042(4)
E1	$1^- \rightarrow 2^+$	0.0085	0.0077(7)
E2	$3^- \rightarrow 2^+$	0.0063	0.0081(16)
E2	$3^- \rightarrow 4^+$	0.0089	0.0082(16)
E3	$3^- \rightarrow 0^+$	8.87	14(2)

In Fig. 2, the QO potential shapes corresponding to the model parameters for  $^{152}\text{Sm}$  are plotted. The left plot represents the full potential shape, whereas the right one illustrates the corresponding effective potential for  $\beta_2 > 0$  with the built-in infinite wall at  $\beta_2 = 0$ . We see that now the full 2DQOM solution suggests a QO potential the bottom of which is not ellipsoidal but possesses single quadrupole and octupole minima. The right plot visualizes the effective oscillation of the nuclear shape between the positive and negative  $\beta_3$  minima with a motion around the zero-deformation core and simultaneous tunneling through a 2D potential barrier. At the same time, the obtained (test) potential shape provides model estimates for the quadrupole deformation  $\beta_2 \sim 0.37$  (somehow overestimated) and for the octupole deformation  $\beta_3 \sim 0.09$  (quite reasonable) in  $^{152}\text{Sm}$ .

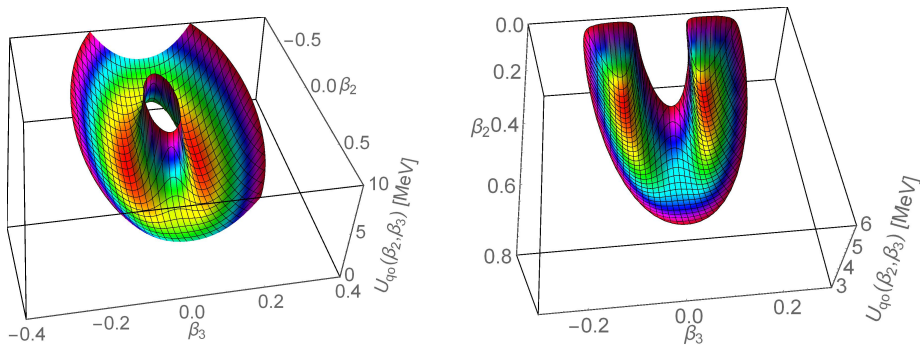


Fig. 2. (Color on-line) 2DQOM model shapes for the full (left) and the effective ( $\beta_2 > 0$ ) (right) QO potential obtained for  $^{152}\text{Sm}$ .



## 5. Conclusion

We found that the analytic CQOM wave functions are suitable to diagonalize the unconstrained QO Hamiltonian in the solution of the full 2D problem for axial QO vibrations and rotations of nuclei. The test calculation for  $^{152}\text{Sm}$  shows that the fits of the unconstrained parameters considerably improve the model description of the yrast APB with the attendant transition probabilities. Also, in this way, the potential shape is unambiguously determined providing model estimates for the possible QO deformation modes. This result encourages the application of the full 2DQOM approach to other nuclei as well as the consideration of non-yrast APB and QPD spectra.

This work has been supported by the Bulgarian National Science Fund under contract No. DFNI-E02/6.

## REFERENCES

- [1] P.A. Butler, W. Nazarewicz, *Rev. Mod. Phys.* **68**, 349 (1996).
- [2] N. Minkov *et al.*, *Phys. Rev. C* **73**, 044315 (2006).
- [3] N. Minkov *et al.*, *Phys. Rev. C* **76**, 034324 (2007).
- [4] N. Minkov *et al.*, *Phys. Rev. C* **85**, 034306 (2012).
- [5] N. Minkov *et al.*, *Phys. Rev. C* **88**, 064310 (2013).
- [6] N. Minkov, S. Drenska, M. Strecker, W. Scheid, *J. Phys. G: Nucl. Part. Phys.* **37**, 025103 (2010).
- [7] N. Minkov, *Phys. Scr.* **T154**, 014017 (2013).
- [8] <http://functions.wolfram.com/Polynomials/LaguerreL3/21/ShowAll.html>
- [9] <http://www.nndc.bnl.gov/ensdf/>
- [10] [http://www.nndc.bnl.gov/nudat2/indx\\_adopted.jsp](http://www.nndc.bnl.gov/nudat2/indx_adopted.jsp)
- [11] T. Kibedi, R.H. Spear, *At. Data Nucl. Data Tables* **80**, 35 (2002).